IEEE Access
Multidisciplinary | Rapid Review | Open Access Journal

Received April 23, 2021, accepted May 24, 2021, date of publication May 28, 2021, date of current version June 8, 2021.

Digital Object Identifier 10.1109/ACCESS.2021.3084620

Wheelchair Automatic Docking Method for Body-Separated Nursing Bed Based on Grid Map

YUDI ZHU, (Member, IEEE), QIAOLING MENG, (Member, IEEE), HONGLIU YU, (Member, IEEE), HAITAO WANG, (Member, IEEE), JIE HU, (Member, IEEE), PING LI, (Member, IEEE), AND BINGSHAN HU, (Member, IEEE)

Rehabilitation Engineering and Technology Institute, University of Shanghai for Science and Technology, Shanghai 200093, China
Shanghai Engineering Research Center of Assistive Devices, Shanghai 200093, China
Key Laboratory of Neural-Functional Information and Rehabilitation Engineering of the Ministry of Civil Affairs, Shanghai 200093, China

Corresponding author: Hongliu Yu (yhl98@hotmail.com)

This work was supported by the National Key Research and Development Program of China under Grant 2020YFC2005800.

ABSTRACT To improve the mode and precision of wheelchair/nursing-bed automatic docking, a novel central embedded wheelchair/nursing-bed automatic docking method based on grid map is proposed. Firstly, Laplace operator and Iterative Closest Point (ICP) algorithm are used to filter and match Lidar point cloud, and the linear features of V-shaped artificial landmark are fitted by Split-merge method and least square method. Then Extended Kalman Filter (EKF) is used to fuse Inertial Measurement Unit (IMU) and odometer data to realize the localization of the bed and wheelchair. Meanwhile, the grid map is used for path planning. Based on the center-line of the two rear wheels and the angular bisector of V-shaped artificial landmark, the wheelchair pose is adjusted in real-time to ensure that the wheelchair gradually approaches the bed along the angular bisector of V-shaped artificial landmark. The yaw angle is reduced by using the improved Proportion Integration Differentiation (PID). 9 sets of experimental data, ie. (x, y, θ) were collected at different starting positions during the docking process. The results show that the yaw angle of the wheelchair during the docking process is controlled within 2.5°, and the distance deviation between the final position and the ideal position of the wheelchair after docking is controlled within 0.02m. In the case of light interference with different luminous fluxes, the docking can still maintain good performance. The proposed docking algorithm has the robust performance of rapid response and low steady error, which can greatly improves the self-care ability of the bedridden elderly, and reduces the labor intensity of the nursing staff.

INDEX TERMS Intelligent wheelchair/nursing-bed system, automatic docking, V-shaped artificial landmark, path planning, grid map.

I. INTRODUCTION

According to the data of the National Bureau of Statistics, the population of China aged 60 and above is 253.88 million by 2019, accounting for 18.1%. Among the 253.88 million elderly people, the population of 65 and above is 176.03 million, accounting for 12.6%. In 2050, China's elderly population will reach up to 35%, and the aging speed has been faster than the speed of economic development [1]. For the bedridden elderly and the disabled, most nursing beds on the market have met the basic functions of turning over, lifting the back, and lifting the legs to reduce the burden on caregivers. Furthermore, with the improvement of nursing needs, the problem of self-care of patients during bedridden needs to be solved [2]. Many scientific research institutions have begun to develop body-separated nursing beds that can realize autonomous navigation and automatic docking. Ren *et al.* [3] adopted the visual docking method based on the specific artificial landmark, used the intelligent image processing system to analyze the data collected by the camera behind the wheelchair to locate the bed, and finally drove the motor to complete wheelchair/nursing-bed automatic docking. Li *et al.* [4] adopted the docking method based on the fusion of vision and ultrasonic wave, and determined the horizontal position of the bed center and the distance from the wheelchair using the manual calibration plate, the visual sensor and the ultrasonic sensor to realize the automatic docking. Ye *et al.* [5] took the differential drive intelligent

The associate editor coordinating the review of this manuscript and approving it for publication was Pedro Neto.

wheelchair as the research object, and realized the automatic docking between the intelligent wheelchair and the U-shaped bed by using visual servo control technology.

At present, most nursing beds are using side-entry docking, but nursing beds with side-entry docking cannot help patients to turn over. Bed-ridden patients who do not often turn over will produce bedsores. In addition, when the patient's body is moved to the side of the bed, it causes secondary injury to the patient. In terms of the existing wheelchair/nursing-bed docking methods, ultrasonic and infrared ranging sensors provide less depth information, causing higher-precision docking tasks are often difficult to complete; visual-based wheelchair/nursing-bed docking methods require preset standard points in the environment and the installation of visual sensors requires a better lighting environment [6]. This paper presents an automatic docking method of the wheelchair and U-shaped bed by using Lidar. There is a Lidar behind the wheelchair and a V-shaped artificial landmark under the bedside frame. According to the deviation between the centerline of the two rear wheels and the angle bisector of V-shaped artificial landmark, the system constantly judges whether it has deviated from the path and makes adjustments. According to the real-time position of the wheelchair obtained by multi-sensor fusion based on EKF, the path is planned through the grid map, and the PID is used to ensure the accuracy of the wheelchair in the docking process. The results showed that the distance error was less than 0.02m, and the yaw angle is less than 2.5°. The main contributions of this paper are as follows.

1) This paper applies the docking technology to the nursing bed field in the rehabilitation industry and adopts the docking method based on the U-shaped bed, which retains the automatic turning function of the nursing bed and reduces the secondary injury of the patient during the movement.

2) This docking method uses Lidar and V-shaped artificial landmark to complete the docking task. The Lidar mapping area is larger and the image is clearer. It can also use the prior knowledge of V-shaped landmark to increase the robustness of the docking. In the case of light interference, good performance can still be maintained.

3) Due to the modular design, the docking method has strong portability, greatly improves the self-care ability of the bedridden elderly, and reduces the labor intensity of the nursing staff.

II. METHODS

A. IMPLEMENT OF WHEELCHAIR/NURSING-BED AUTOMATIC DOCKING SCHEME

The docking method uses the Rive function package of ROS to complete the graphic visualization operation and projects the point cloud obtained by Lidar onto the map established by ROS [7]. Lidar is one of the important devices for sensing the environment and using the principle of Lidar ranging and the controller and scanner to image the position and angle of laser emission. In Fig. 1, HOKUYO UST-10LX 2D Lidar

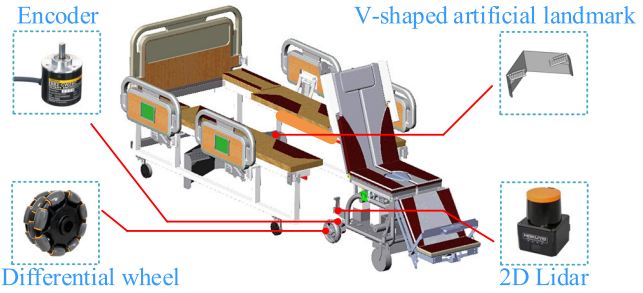

FIGURE 1. The body-separated nursing bed proposed in this paper.

locates the bed and wheelchair by scanning V-shaped artificial landmark. It has 270° measurement range and the scanning interval is 1°, and 270 scanning points will be obtained at a time. By scanning the preset mark point by point, the distance between the emission point and the observation point is calculated, and the feature lines of the preset mark is fitted. The differential wheel and encoder are combined to adjust the pose of the wheelchair. The key technologies are as follows:

1) The line and corner features of the bed model are extracted by postpositive Lidar, and the bed model is matched and located by the improved iterative matching algorithm.

2) Based on the wheelchair kinematics model, a compliant local path planning algorithm of improving the comfort of patients is studied to realize the wheelchair/nursing-bed docking.

B. WHEELCHAIR/NURSING-BED AUTOMATIC DOCKING METHOD

The main process of wheelchair/nursing-bed docking algorithm is Lidar point cloud data fitting (the point cloud is a large number of point sets expressing the spatial distribution and surface features of the target in the same spatial reference frame), local positioning and path planning [8]. Besides, considering the safety and stability factors, the successful docking should meet three conditions:

1) The relative position relationship between the nursing bed and wheelchair was identified;

2) Data that can be identified, processed, and transmitted;

3) The accuracy is high enough (the error range can be controlled within 0.02m, and the yaw angle can be controlled within 2.5°).

To improve the accuracy and speed of automatic docking, we use the bilateral right angle structure as V-shaped artificial landmark in the bottom frame of the bedside side. The whole process is shown in Fig. 2.

1) LIDAR POINT CLOUD FILTERING

In the process of using Lidar to obtain a large number of point cloud, it is easy to be affected by the surrounding environment, equipment accuracy, and human factors. There will be some error points in the point cloud, which are called noise point cloud [9]. The Laplace algorithm is used to filter the Lidar point cloud, and the Laplace operator is used to

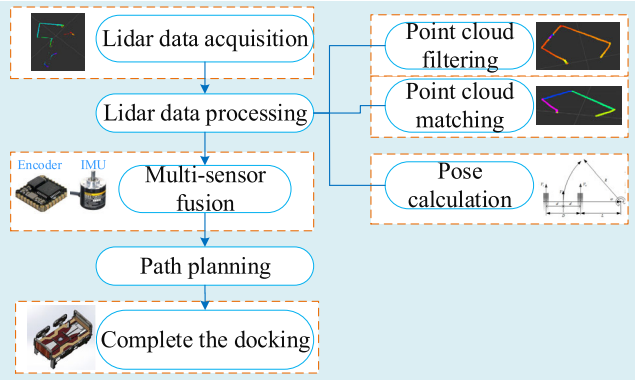

FIGURE 2. System scheme diagram of docking method.

calculate each vertex of the Lidar point cloud. Then the high-frequency data points are diffused into the neighborhood and gradually matched with the neighborhood point cloud [10].

2) LIDAR POINT CLOUD MATCHING

Lidar point cloud matching is mainly used to locate the bed and wheelchair, usually using efficient and accurate ICP for matching[11]. Because the wheelchair can only move on the ground during the docking process, the rotation relative to the Z axis(vertical axis) is not considered in the world coordinate system. In Δt time, the Lidar scans V-shaped artificial landmark, and the two groups of data scanned before and after are recorded as set M and set N respectively. According to the scanning order, set M and set N are divided into k groups averagely. If the point cloud matching rate of each group (the matching rate is the number of successful point cloud in the group divided by the total number of point cloud in the group) reaches the set threshold, the point cloud matching is successful [12]. The given threshold is related to the Lidar resolution. The effective range of the Lidar is 10m and the angular resolution is 0.25°. Therefore, the minimum distance between adjacent scanning points is $2 \times 10 \times \sin(0.125^o)$ =0.0436m, and then set threshold is 0.0436m. To ensure the accuracy of point cloud matching, δ and ζ set to 95% [13]. The specific algorithm flow is shown in Fig. 3.

3) FEATURE EXTRACTION OF V-SHAPED ARTIFICIAL LANDMARK

Although many signs can be used as the landmark, the installation of artificial landmark which like an isosceles right triangle in the middle of the bed provides sufficient corner and straight-line features for Lidar positioning. In the positioning process, the current relative pose between the bed and wheelchair can be obtained by determining the two-sided linear structural equation and solving the corner position, and then controlling the wheelchair to dock. In addition, the results obtained can be verified by using a priori knowledge with 90°, which greatly simplifies the difficulty of Lidar data processing and improves the robustness of the positioning algorithm. In order to obtain the characteristic lines of

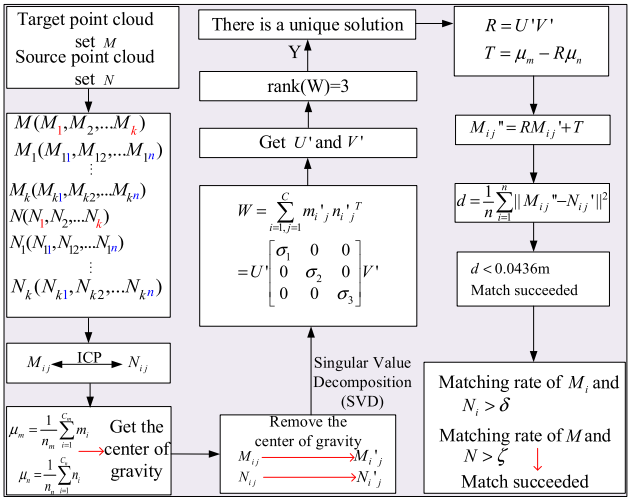

FIGURE 3. Flow chart of ICP point cloud matching.

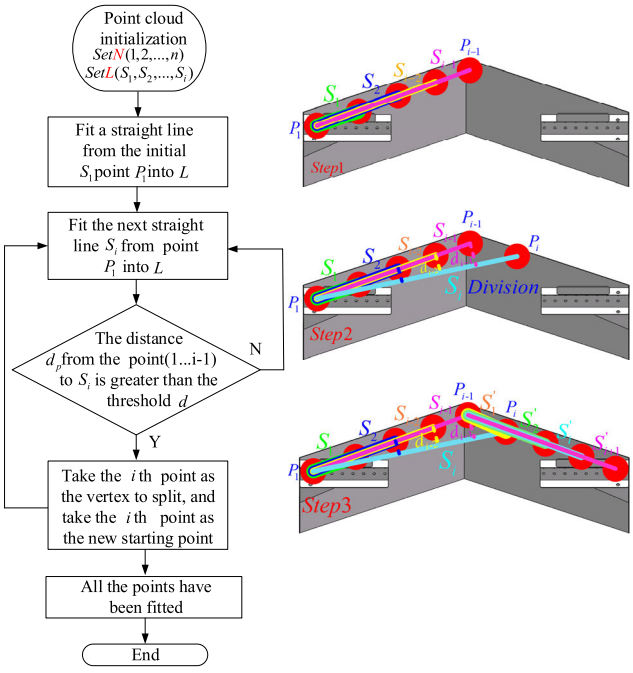

FIGURE 4. Flow chart of Split-merge method.

V-shaped artificial landmark, Split-merge method is used to extract the features of Lidar point cloud, and the problem of finding a plane in 3D space is transformed into the problem of finding a straight line in 2D space [14]. Through the manual selection method, we analyze the graphics to be fitted. V-shaped artificial landmark to be fitted is an isosceles right triangle with a side length of 0.6m, so the distance threshold is set to 0.6m [15]. The algorithm flow of the Split-merge method is shown in Fig. 4.

As shown in Fig. 5, the L_0 and L_1 sides of V-shaped artificial landmark are fitted with the least square method to obtain the angle bisector L_P of V-shaped artificial landmark and the angle θ between the wheelchair and the target point, which are

TABLE 1. Definition of design equation symbols in Fig. 4.

Symbol	Definition
S_i	Fitting line segment of point cloud
L	Collection of S
d	Distance threshold of Lidar
d_p	Distance from the point to the fitted line

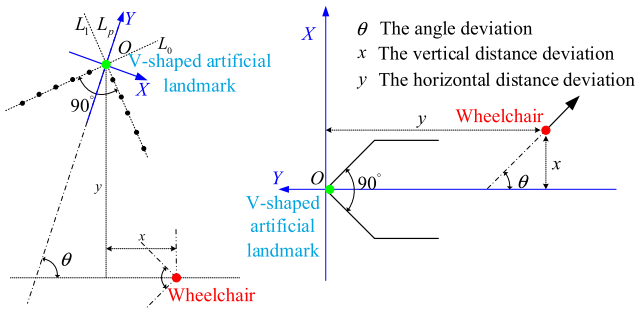

FIGURE 5. Positioning of the relative position of the wheelchair.

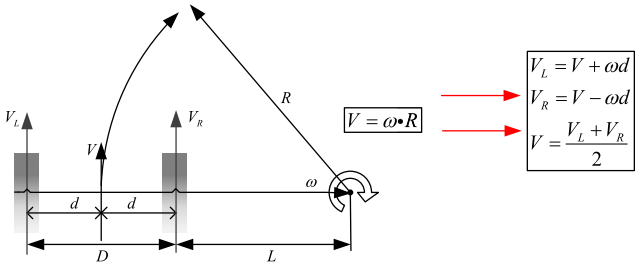

FIGURE 6. Kinematic analysis of two-wheel differential structure.

TABLE 2. Definition of design equation symbols in Fig. 6.

Symbol	Definition
V	Wheelchair velocity
ω	Angular velocity
R	Turning radius
D	Distance between the two wheels
L	Turning radius of the right wheel
V_L	Left wheel speed
V_R	Right wheel speed

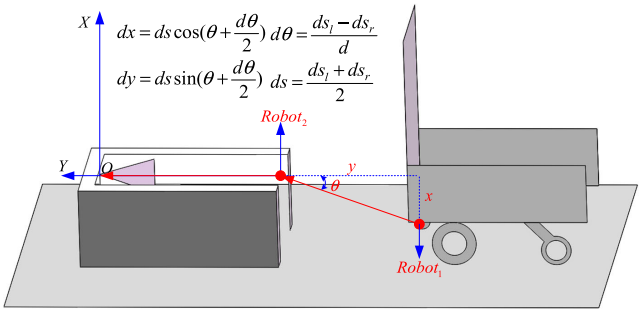

FIGURE 7. Differential motion of wheelchair.

TABLE 3. Definition of design equation symbols in Fig. 6.

Symbol	Definition
d	Half the distance between two wheels
ds	Distance of wheelchair
ds_l	Distance of left wheel
ds_r	Distance of right wheel

important parameters for the successful docking. The relative posture between the intelligent wheelchair and the bed can be obtained, and wheelchair/nursing-bed automatic docking can be realized through the motion control algorithm.

4) ANALYSIS OF WHEELCHAIR MOTION MODEL

The perception and positioning of the wheelchair are directly related to the quality of mapping and docking accuracy. According to the change of the photoelectric encoder pulse in the sampling period, the odometer is mainly used to calculate the trajectory of the robot, the distance and the angle of the wheel relative to the ground. The trajectory is composed of positions, including coordinates and angles [16]. For the two-wheel differential mobile robot, the pose change of the robot is calculated by detecting the curvature of the wheels with the odometer. The analysis of the two-wheel differential structure is shown in Fig. 6.

According to (1), the position of the wheelchair at the previous moment is used to estimate the position of the wheelchair at the next moment.

$$\begin{bmatrix} x' \\ y' \\ \theta' \end{bmatrix} = \begin{bmatrix} x \\ y \\ \theta \end{bmatrix} + \begin{bmatrix} \cos\theta & -\sin\theta & 0 \\ \sin\theta & \cos\theta & 0 \\ 0 & 0 & 1 \end{bmatrix} \begin{bmatrix} dx \\ dy \\ d\theta \end{bmatrix} \quad (1)$$

The motion model of the wheelchair is shown in Fig. 7. The encoder data de_l and de_r are obtained through the bottom control system. ds_l and ds_r can be calculated according to (2), where r is the turning radius and t is the motor transmission ratio.

$$ds_l = \frac{2\Pi r de_l}{8000t}, \quad ds_r = \frac{2\Pi r de_r}{8000t} \quad (2)$$

5) MULTI-SENSOR DATA FUSION BASED ON EKF

The docking method uses the Gmapping function package in ROS to create a grid map based on the received Lidar data and the odometer information. The improved RBPF (Rao-B- lackwellized Particle Filters) particle filter algorithm is used to solve the problem of particle dissipation caused by frequent resampling [17]. There is no real-time calibration

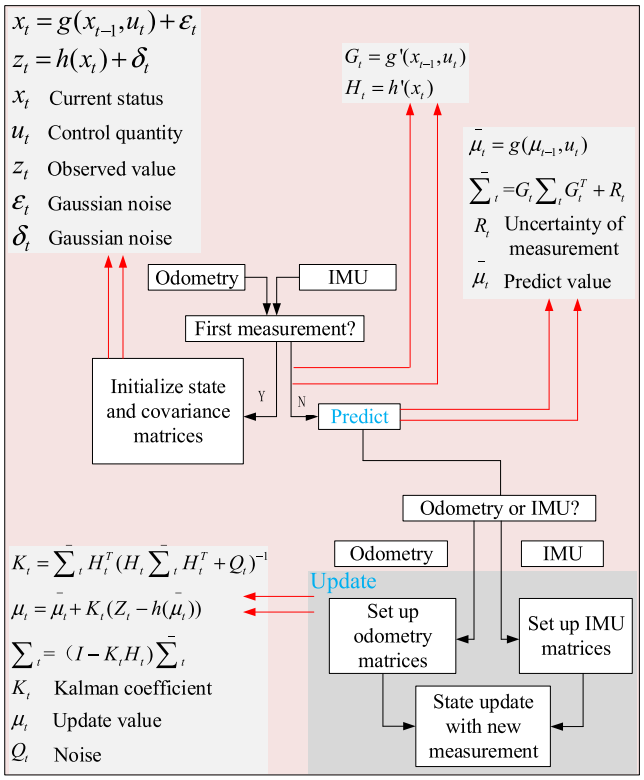

FIGURE 8. Flow chart of multi-sensor fusion.

to the wheel odometer derived from the geometric model. Hence, the error is always accumulated in the results. The docking method obtains the acceleration, the angular velocity and the Euler angle of the wheelchair in the IMU through the ROS, publishing the data to the data fusion node through the Topic to further improve the accuracy of motion estimation. Then EKF is used to fuse the data of the odometer and IMU, which makes the positioning system has higher accuracy and robustness [18]. The specific steps are shown in Fig. 8.

After updating the observation equation of the first sensor system, the obtained observation μ_t and system covariance matrix $\sum t$ are used as the system prediction state quantity $\overline{\mu}_t$ and system prediction covariance matrix $\overline{\sum} t$ in the next sensor updating process. The above process is repeated until the fusion outputs μ_t and $\sum t$ of the last sensor. The two values are used in the next iteration of the prediction process.

III. PATH PLANNING OF WHEELCHAIR DOCKING

Path planning is to find the shortest and optimal path according to certain performance indicators (such as distance, time, etc.). In the research fields of mobile robots, path planning is one of the key technologies for robots to achieve autonomous motion [19]. The core of path planning is path planning algorithm. The most commonly used path planning algorithms include free-space method, graph search method, and grid map. The grid map divides the robot's working environment into cell grids of the same size and shape. These cell grids are connected to each other without overlap, and the occupied

TABLE 4. Parameter definition of Gmapping.

Symbol	Definition	Set value
map.info.resolution	Represents the number of cells contained in 1m	0.05m/pixel
map.info.width	Pixels contained in the initial width of the grid map	20pixel
map.info.height	Pixels contained in the initial height of the grid map	20pixel
occupied_thresh	Pixels larger than the threshold are considered fully occupied	0.65pixel
free_thresh	Pixels less than the threshold are considered completely idle	0.196pixel
mapParams.log_free	Update amount of idle value	-1 pixel
mapParams.log_occ	Update amount of occupancy value	2 pixel

value of each cell is 0 and 1 respectively, representing the occupied state and the idle state respectively [20]. To improve the quality and efficiency of path planning, this paper uses the grid map to solve the wheelchair/bed automatic docking and studies the path planning problem.

A. OCCUPY GRID MAP CONSTRUCTION ALGORITHM

The odometer of the mobile wheelchair indicates the position of the wheelchair in the world coordinate system at all times. The Gmapping function package of ROS uses the odometer data as the control input, and combines with the Lidar to map the indoor environment in real time. Gmapping creates a map using an occupancy grid map construction algorithm, which requires less calculation in small scenes, higher map accuracy, and lower requirements for Lidar scanning frequency [21]. First, according to a frame of Lidar data and the corresponding robot pose, the cell number of the robot position is calculated. ROS get the cell serial number of the cell in the pixel coordinate system in each laser click, and change the cell number of the current robot pose. The serial number is connected with the cell serial number of the laser scanning point in a straight line to find all the idle cell serial numbers, Gmapping traverse all the idle cells, update the idle cell status, and finally update the cell status in the laser scanning click. There are many parameters of Gmapping, the setting of several important parameters is shown in Table 4 [22].

The grid map divides the environment map into many cells, and different values are stored in the cell to indicate different states of the cell [23]. The grid map of ROS uses white to represent leisure which indicates a passable area, with a stored value of 0; Black represents occupied which indicates an unpassable area with the stored value is 100; Gray represents an unknown state, which stores value is -1. The color of each small cell in the grid map represents the probability of the cell being occupied. The darker color indicates the higher occupancy rate [24]. The range is [0,100]. The coordinates of each cell in the grid map correspond to a coordinate of the actual map. The coordinates of a certain point (x, y) in the actual map, and the coordinates in the corresponding grid map are $[x^*map.info.width + y]$. The resolution of the grid

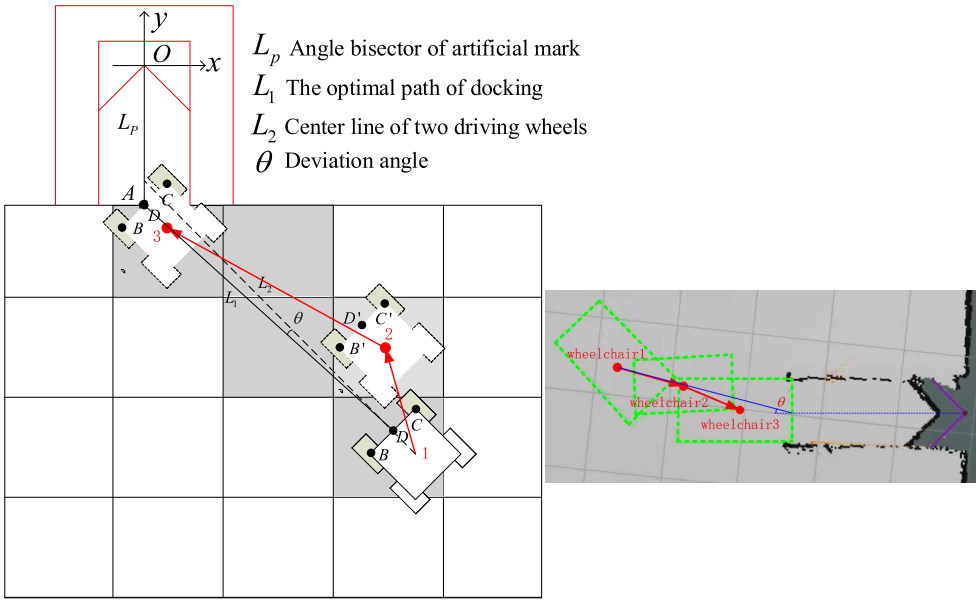

FIGURE 9. Schematic diagram of path planning.

map is set to 0.05, which means that there are 20 × 20 cells within 1m2, and each cell takes up a byte of memory. The smaller cell means the larger memory and the slower running time. We control the size of the cell on the premise of ensuring accuracy to make the wheelchair more sensitive. For the active area of 80m2, the amount of memory and calculation needed to build the map at the selected resolution is not very large, which can meet the daily use.

B. WHEELCHAIR POSTURE ADJUSTMENT BASED ON GRID MAP

In the process of path planning, the map is divided into multiple cells to filter out the infeasible cells. The size of the cell is matched with the moving step length of the robot, and each cell is used as a basic unit to determine a starting point and an ending point. First, connect the start point and the end-point with a straight line, record the grid cells that the line passes through, and mark them with gray in the grid map. Then search the next grid cell that the wheelchair will pass through according to the optimal path, adjust the wheelchair posture to make the wheelchair move to this cell at the shortest distance. Repositioning the wheelchair, reconnecting two points and to determine the next cell, and repeat the above steps until the wheelchair reaches the target position [25]. The specific method is shown in Fig. 9.

(1) Determine the starting position and target position in the grid map. The starting position is the cell where the vertex D of the median line of the two driving wheels BC behind the wheelchair is located. The target position is the intersection A between the angle bisector L_P of V-shaped artificial landmark and the bed frame.

(2) Solve the median line L_2 of BC and the median line L_1 of AD. L_1 is the shortest distance between the wheelchair and the target point A, and the angle between L_1 and L_2 is judged. If θ is not 0°, the wheelchair posture will deviate from the target point A. The two-wheel differential structure is adopted to adjust the rotation speed V_L and V_R of left and right wheels behind the wheelchair, and the wheelchair posture to make the left wheel move to $B'(x'_B, y'_B)$ position. The right wheel moves to the position $C'(x'_C, y'_C)$, the median line of B' and C' coincides with L_1, so that θ is 0°.

(3) Adjust the position and posture of the wheelchair to position B' and C'. For the positions of the bed and wheelchair known in the world coordinate system, the initial positions of the left and right wheels of the wheelchair is set to

$$A(x_A, y_A), B(x_B, y_B), C(x_C, y_C),\ D(\frac{x_B + x_C}{2}, \frac{y_B + y_C}{2}),$$

we get the coordinates of $B'(x'_B, y'_B)$ and $C'(x'_C, y'_C)$. According to the linear equation of AD, the slope k_1 is obtained by (3).

$$k_1 = \frac{y_B + y_C - 2y_A}{x_B + x_C - 2x_A} \tag{3}$$

According to the linear equation of BC, the slope k_2 is obtained by (4).

$$k_2 = \frac{y'_B - y'_C}{x'_B - x'_C} \tag{4}$$

Let the distance between the left wheel and the right wheel to the center point D be d. If AD is perpendicular to $B'C'$, then we can get (5) and (6).

$$d = \frac{|\frac{y_B+y_C-2y_A}{x_B+x_C-2x_A}x'_B + y'_B + y_A - \frac{y_B+y_C-2y_A}{x_B+x_C-2x_A}x_A|}{\sqrt{(\frac{y_B+y_C-2y_A}{x_B+x_C-2x_A})^2 + 1}} \tag{5}$$

$$k_1 \cdot k_2 = -1 \tag{6}$$

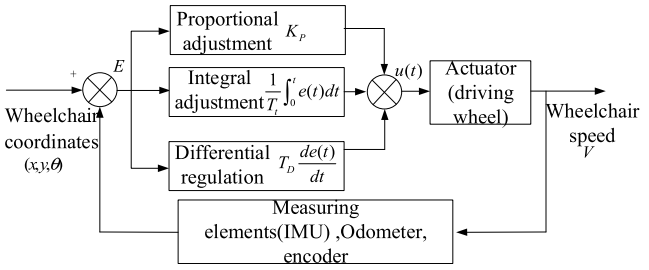

FIGURE 10. PID control structure block diagram.

When the wheelchair adjusts its posture, turn both wheels at point D, then we can get (7) and (8).

$$\frac{x_B + x_C}{2} = \frac{x'_B + x'_C}{2} \tag{7}$$

$$\frac{y_B + y_C}{2} = \frac{y'_B + y'_C}{2} \tag{8}$$

The coordinates of B' and C' can be obtained from (5) (6) (7) (8).

(4) After adjusting the posture of the wheelchair, drive the wheelchair to move to the next grid cell nearby along the median line of BC. But there may be deviation during the movement. After the wheelchair enters the next cell, reposition the wheelchair and repeat the above steps until the coordinates of point A and point D coincide.

(5) After the coordinates of point A and point D coincide, adjust the wheelchair posture to make the median line BC coincide with the angle bisector L_P of V-shaped artificial landmark. The wheelchair gradually approaches the artificial landmark along the angle bisector until the docking is completed.

C. PID FOR REDUCING WHEELCHAIR JITTER

The PID is a closed-loop control algorithm, which uses feedback algorithm to continuously calculate the proportion, differential and integral of the error value, and continuously correct wheelchair coordinates of the input value, to ensure the stability of docking and improve the docking accuracy [26]. To improve the stability and docking accuracy of the wheelchair during the docking process, the PID is used to reduce the yaw angle such as jitter and sideslip during movement.

The docking method adopts the two-wheel differential structure. The two rear wheels are used as the driving wheels, which have independent control speeds. They are combined with two universal wheels to realize the position and posture control of the wheelchair through different speeds of the given driving wheels. In order to control the wheelchair to move at a stable speed V according to a specific trajectory, the PID is added to the two driving wheels to make the movement of the left and right wheels in a dynamic balance. As shown in Fig. 10, take the error E between the expected value (x, y, θ) and the actual value of the wheelchair coordinate as input, and proportional, integral and derivative operations are superimposed to control the actuator to adjust the azimuth angle of the wheelchair. The current distance and position are sensed by measuring components (IMU), odometer and encoder. Obtaining the current position coordinates of the wheelchair (x', y', θ'). The computer control, a kind of sampling control which only calculates the control quantity based on the deviation of the sampling time, cannot continuously output the control quantity like analog control for continuous control. According to the sampling time of the motor encoder, we set the sampling time to 100ms, calculate the coordinate error between the current value and the expected value, form the PID closed-loop feedback through the measuring components, and gradually adjust the yaw angle of the wheelchair so that the wheelchair can move stably.

IV. RESULTS

When the Lidar receives the docking signal, the wheelchair moves to the bedside, and then through Lidar data acquisition, Lidar filtering, Lidar feature extraction, coordinate system conversion, intelligent wheelchair automatic control, the accurate docking of the bed and chair is completed [27]. To verify the effectiveness and feasibility of our docking method, we analyzed and verified the whole process of wheelchair/nursing-bed docking. First, the wheelchair was removed from the bed by using the automatic navigation function. Then the docking experiment is started at a speed of 0.1m/s while the wheelchair is a certain distance away from the bed. The trajectory planning of wheelchair is carried out in the field of idle cell, and the yaw angle is gradually adjusted for real-time planning. The current position and speed of wheelchair are calculated according to the encoder values of the two driving wheels, and the trajectory is converted into the world coordinate system. The trajectory is published to ROS by SPI (Serial Peripheral Interface) communication to provide data for SLAM (Simultaneous Localization and Mapping) algorithm [28]. At the same time, the yaw angle of the wheelchair in the process of moving is recorded, and the positioning accuracy of the wheelchair in the docking process is obtained according to the yaw angle.

We conducted docking experiments in an 80m^2 laboratory, where the laboratory light environment was well. The process of setting up the environment map based on the distributed deployment, we used a remote computer to control the intelligent wheelchair to move indoors, and set the direction keys of the keyboard as the speed controller and steering controller separately, then realized the establishment of the 80m^2 grid map of the whole laboratory. In the docking process, the intelligent wheelchair realizes the detection of obstacles, the planning of the layout path and the adjustment of the global path, finally completes the docking task. As shown in Fig. 11 (a), the intelligent wheelchair receives the parking command and starts to move near the bed. The wheelchair is positioned based on grid map, and then the PID is used to reduce the yaw angle during the movement of the wheelchair. As shown in Fig. 11(b), the wheelchair constantly adjusts the deviation between the current position and the ideal position to prepare

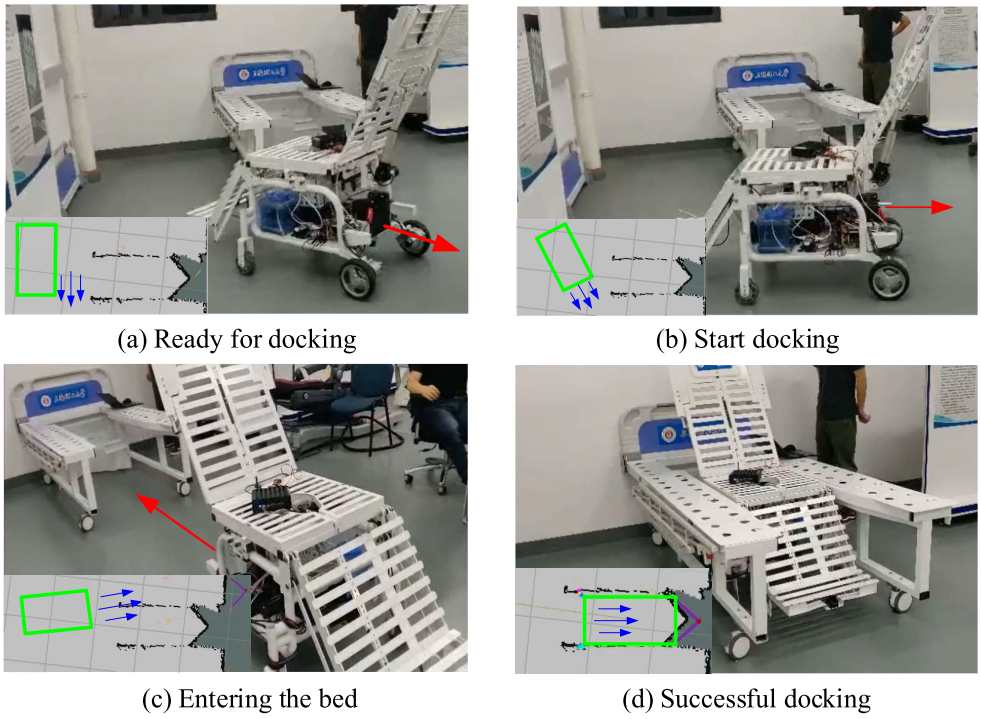

FIGURE 11. Automatic docking process.

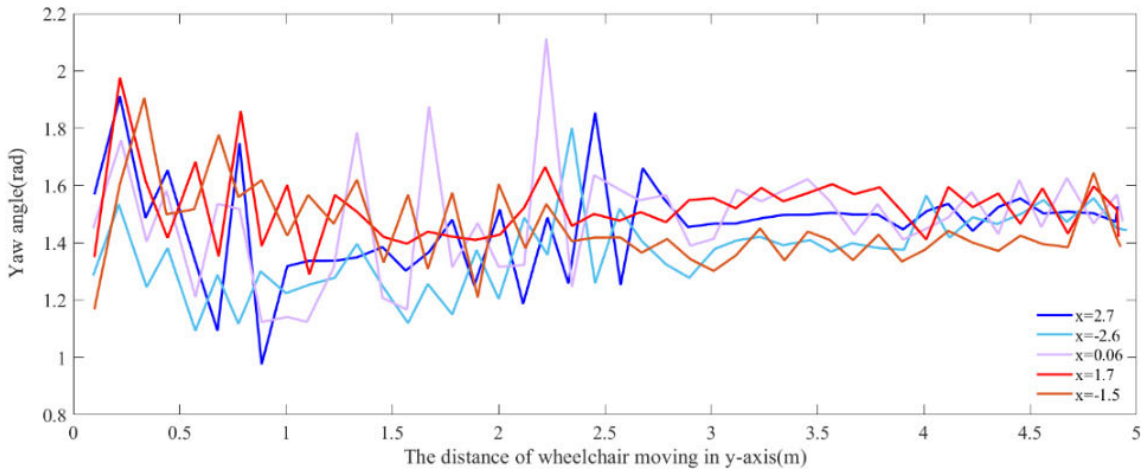

FIGURE 12. Process curve of deviation angle.

to enter the bed. As shown in Fig. 11(c), the wheelchair adjusts the angle based on path planning so as to enter the bed optimally. As shown in Fig. 11(d), the wheelchair has been embedded in the bed, and then move in a straight line and dock smoothly with the bed by driving the rear wheels. After successful docking, the deviation between the final position and the ideal position is controlled within 0.02m. We make 9 experiments, which take 9 sets of the initial position of the wheelchair with the speed of 0.1m/s. The optimal path is planned by the grid map during backward docking. It can be seen from Table 4 that the wheelchair can dock with the bed successfully in nine cases. The average error and the maximum error of Δx, Δy and $\Delta\theta$ are within the controllable range, which indicates that the method is reliable.

We selected five sets of representative data, Matlab is used to fit the correlation curve of the initial pose (2.7, −5, 28°) (1.7, −5, 20°) (0.06, −5, 1°) (−1.5, −5, 17°) (−2.6, −5, 27°) in the process of automatic docking. Fig. 12 shows the yaw angle between the median line of the two rear wheels of the wheelchair and the optimal path, and Fig. 13 shows the trajectory of the wheelchair in the docking process.

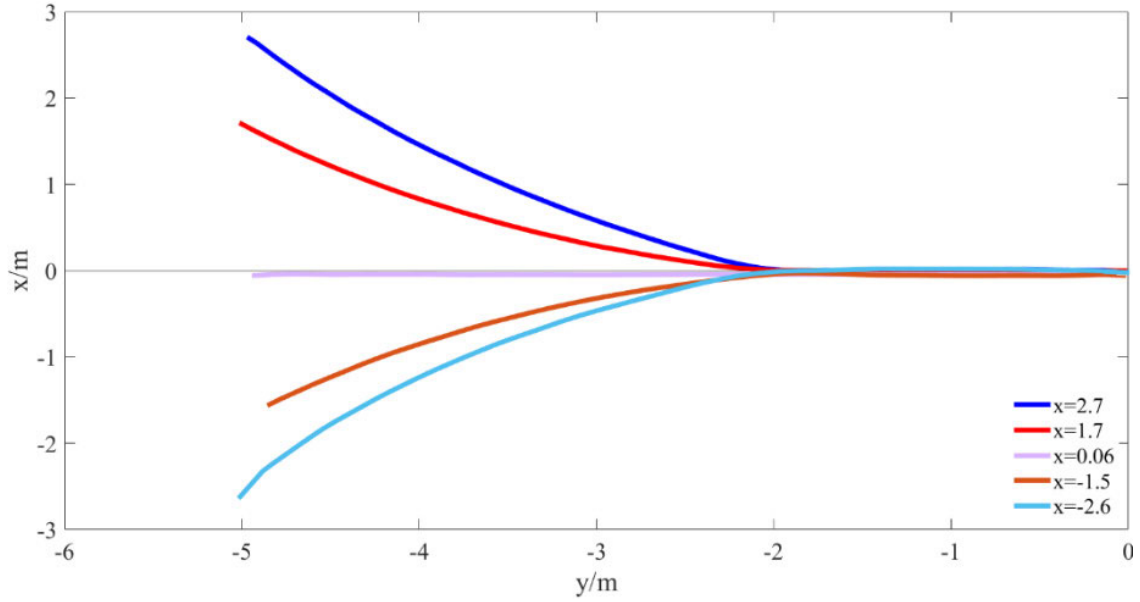

FIGURE 13. Track curve of wheelchair docking process.

TABLE 5. Automatic docking experiment results.

Initial pose ($x/m, y/m, \theta°$)	Terminal pose ($x/m, y/m, \theta°$)	Average errors			Maximum errors		
		$\Delta x(m)$	$\Delta y(m)$	$\Delta\theta(°)$	$\Delta x(m)$	$\Delta y(m)$	$\Delta\theta(°)$
(4.5,-7.2, 32)	(0.012,0.007,1.4)	0.010	0.015	1.5	0.016	0.018	2.4
(3.2,-4.1,38)	(0.011,0.012,1.5)	0.012	0.013	1.2	0.015	0.015	2.2
(2.7,-5,28)	(0.009,-0.008,1.5)	0.009	0.013	1.5	0.018	0.014	1.9
(1.7,-5,20)	(-0.013,0.006,1.2)	0.012	0.008	1.6	0.017	0.012	2.0
(0.06,-5,1)	(0.012,0.007, 1.9)	0.011	0.007	1.6	0.016	0.015	2.1
(-1.5,-5,17)	(-0.006,0.008, 1.1)	0.004	0.006	1.4	0.007	0.009	1.9
(-2.6,-5,27)	(0.017,-0.015,1.3)	0.015	0.013	1.3	0.018	0.014	1.8
(-3.8,-4.9,38)	(-0.013,0.012,1.2)	0.011	0.007	1.2	0.016	0.015	2.2
(-4.0,-6.8,31)	(0.012,0.007,1.9)	0.011	0.007	1.7	0.016	0.015	2.3

Lidar plays an irreplaceable role in the entire SLAM and navigation. First, the pose of the robot can be estimated by matching the Lidar observation data with the grid map. Second, when the robot estimates a more accurate pose, the environment map is established based on the Lidar observation data after the robot has estimated a more accurate pose. Third, the unknown obstacles in the map are detected in the process of robot navigation [29].

The anti- interference ability of ambient light is one of the important indexes to measure the quality of Lidar, and the light intensity may interfere with the data generated by Lidar. We carried out docking experiments under different lighting conditions to observe the robustness of the docking method. The experiment was conducted in a space of 80m^2 and a height of 5m. The light source is fixed in the center of the room. HOKUYO UST-10LX 2D Lidar can work normally in the light environment less than 15000lm, and the docking experiment was conducted at the same starting point using light fluxes of 3000lm, 5000lm and 8000lm as the impact factors to analyze the changes in yaw angle.

The experiments are divided into two groups with starting points A (-1.5, -5, 17°) and B (1.7, -5, 20°), and three light fluxes are used to affect the docking process using xenon lamp flashlights. Comparing the yaw angle generated under a normal environment with the yaw angle with the light flux of 3000lm, 5000lm and 8000lm respectively, the average value and standard deviation of the yaw angle during the docking process is used as an index to analyze the robustness of this docking method.

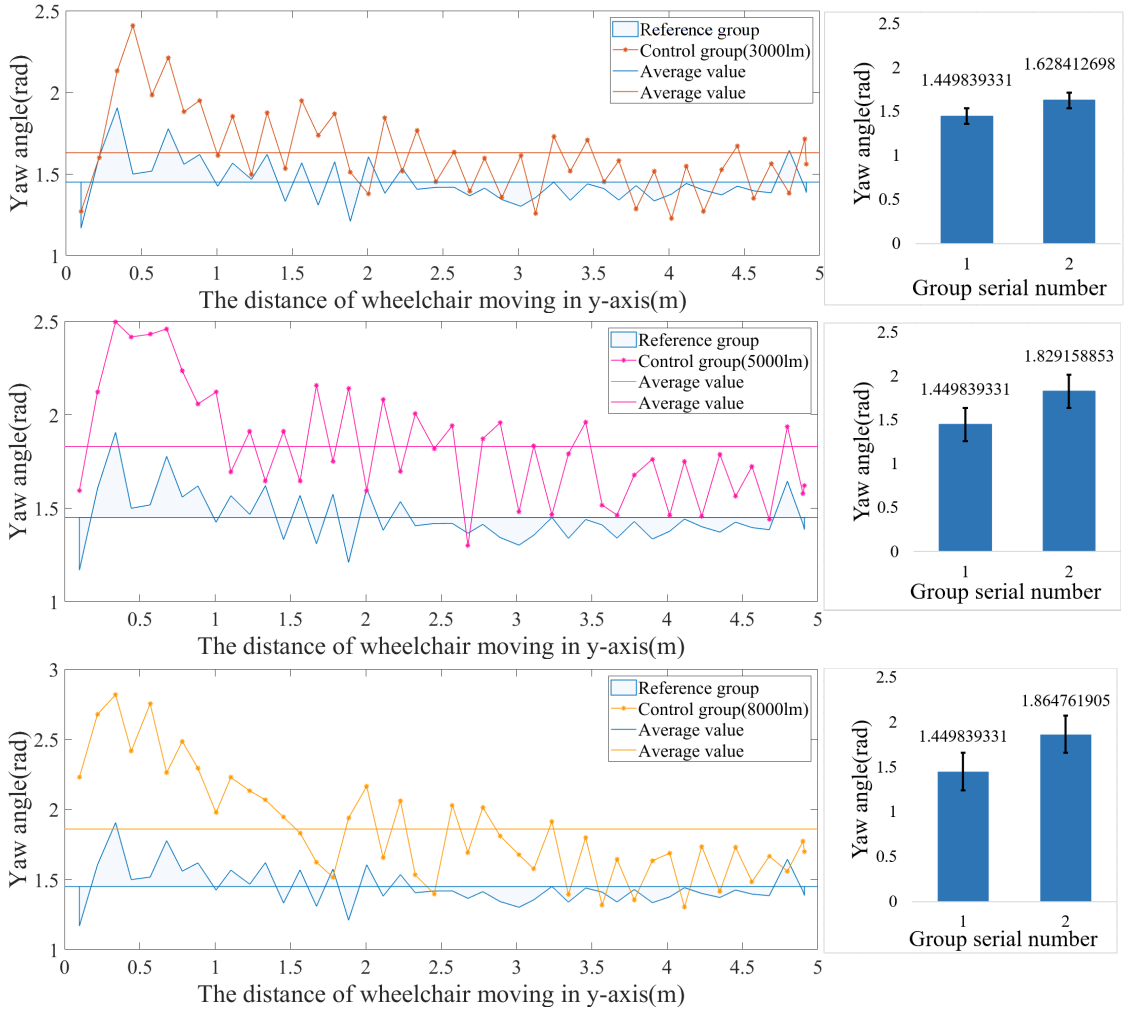

FIGURE 14. The yaw angle comparison chart for starting point A.

Fig.14 is a tendency chart of the yaw angle with the starting point A (−1.5, −5, 17°). Fig.15 is a tendency chart of the yaw angle with the starting point B (1.7, −5, 20°). It can be seen that increasing the influence factor during docking the process will increase the average of the yaw angle. As shown in Fig.14 and Fig.15, the volatility is greater at the beginning of docking, and the yaw angle slowly stabilizes with the increase of wheelchair walking distance, which is also related to the more accurate characteristics of the Lidar to identify objects at a long distance. The greater light flux value means the greater effect on the yaw angle. When the light flux of 8000lm is irradiated, the docking can be done successfully although the yaw angle exceeds 2.5° in individual cases. The required illumination in daily life is about 150lx, and 8000lm can produce 380lx of light in the room of 80m^2. So the stability of this docking algorithm can meet daily use and has good stability.

V. DISCUSSION

The mode and algorithm of Wheelchair/nursing-bed automatic docking will directly affect the accuracy of the docking and user experience, this paper proposed the wheelchair/nursing-bed automatic docking method based on Lidar and V-shaped artificial landmark. Lidar can easily extract straight-line and corner features of V-shaped artificial landmark, and using the prior knowledge with 90° of V-shaped artificial landmark can also improve the docking success rate. The robot technology will be transferred to the healthcare area, and self-care of the bedridden elderly will be realized. It can be seen from the experimental results that the trajectory in the docking process is smooth. In the case of light interference, the yaw angle is also in a controllable range, and the wheelchair can be successfully docked. Meng *et al.* [30] proposed a docking method based on Lidar and force sensor. Firstly, the shape of the bed body is identified according to the Lidar, and the relative posture between the bed and wheelchair is calculated. Then, when the wheelchair is in contact with the bed, the posture of the wheelchair is adjusted according to the feedback signal of the force sensor, and the automatic docking will completed. Because the wheelchair and the auxiliary bed utilize side-entry docking, the bedridden patient can only be assisted to turn over on one side, which will cause a burden to the nursing staff. In contrast, the U-shaped bed docking mode can assist the bedridden patient

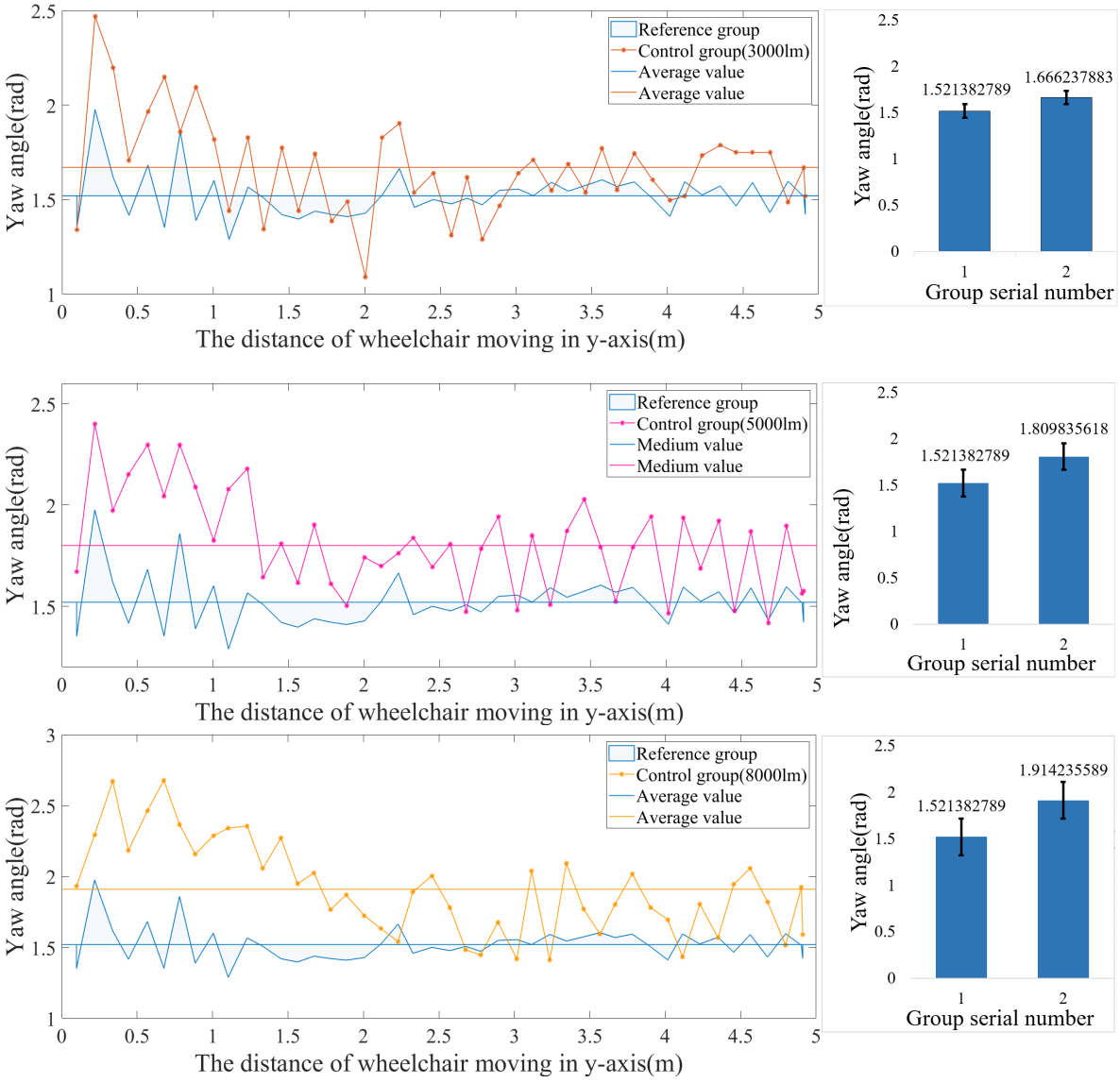

FIGURE 15. The yaw angle comparison chart for starting point B.

to turn over on both sides, greatly improving the bedridden patient's self-care ability, and reducing the occurrence of bedsore and pneumonia. In addition, when the patient is in the middle of the bed, the bed can be converted into a wheelchair without the need to move the patient's body, which can protect the bedridden patient from secondary injury. Li *et al.* [31] proposed an automatic docking method based on vision measurement. The process of the wheelchair/nursing-bed docking is divided into the long-distance guidance stage and the short-range docking stage. In the long-distance guidance stage, a visual acquisition system needs to be installed on the ceiling, which has high requirements for the use environment. In the short range docking stage, when the camera is close to the target, the camera defocus makes the visual positioning docking method ineffective. The experimental results show that the distance deviation of the wheelchair is less than 0.05m and the yaw Angle is less than 2°. The docking method of this paper is based on Lidar which when changing the operating environment, Lidar just needed to rebuild the environment map, and the distance deviation is less than 0.02m and the yaw angle is less than 2.5° after successful docking. In terms of yaw angle, we still have space for improvement. Li *et al.* [32] designed coded road signs that could be recognized under ambient light, and the position and attitude of the robot can be estimated according to the recognized road signs. They analyzed the effect of lamp light in the experiment. Lamp light has a great impact on the recognition process, but the method can deal with most of the challenging situation. They experimented that the forklift was required to pick up the goods shelf at one specified location and carry it to another, the maximum position error is 79.3 mm, the maximum yaw angle is 1.36°. Although the positioning

method based on such road signs is effective, it is necessary to design several different road signs to constitute the road sign positioning system, which will increase the complexity of the extraction of different road signs, this stage has no practical importance in daily use.

VI. CONCLUSION

This paper proposes a method of wheelchair/nursing-bed automatic docking based on Lidar and V-shaped artificial landmark. The docking method can realize the automatic separation and merger between wheelchair and bed. While retaining the function of turning over the nursing bed, reducing the secondary injury of bedridden patients in the transfer process, and greatly improving the self-nursing ability of bedridden patients. Under ambient light condition, the distance deviation and the yaw angle between the final position and the ideal position are controlled within 0.02m and 2.5° after successful docking. Besides, the docking method can still maintain good performance in light interference experiments. But the wheelchair should be first moved to the area near the nursing bed by the autonomous navigation to achieve coarse positioning of the bed and wheelchair after receiving the docking instruction, and then use the postpositive Lidar to scan V-shaped artificial landmark to achieve precise partial positioning, and the docking method can complete the docking well in an effective space. If the wheelchair is far from the bed, the docking success rate is low. Besides, due to the docking method adopts the backward driving method, the turning radius of the wheelchair will be comparatively large. Therefore, we need to study the distance limit between the bed and the wheelchair, combine various point cloud filtering algorithms, change driven mode, select artificial landmarks with an appropriate area, combine with visual control and voice control, and explore a more accurate path optimization algorithms to maximize patient convenience and improve docking success rate.

REFERENCES

[1] P. Newswire, *Population Aging Slower Than Other Countries, Census Bureau Reports*. New York, NY, USA: PR Newswire, Mar. 2016.
[2] Z. H. Zhang, "The market demand and industrial development of Chinese nursing service robot," *Basic Clin. Pharmacol. Toxicol.*, vol. 124, p. 184, Apr. 2020, doi: 10.1111/bcpt.13217.
[3] Y. Ren, W. Zou, H. Fan, A. Ye, K. Yuan, and Y. Ma, "A docking control method in narrow space for intelligent wheelchair," in *Proc. IEEE Int. Conf. Mechatronics Autom.*, Aug. 2012, pp. 1615–1620.
[4] X. Li, X. Liang, J. Fan, and S. Jia, "Position-based visual servo control of intelligent Wheelchair/bed docking," in *Proc. IEEE Int. Conf. Inf. Autom. (ICIA)*, Aug. 2018, pp. 1497–1502.
[5] A. Ye, W. Zou, Z. Xu, T. Lu, and K. Yuan, "Docking control of intelligent wheelchair based on vision," in *Proc. 9th World Congr. Intell. Control Autom.*, Jun. 2011, pp. 214–219.
[6] W. Zou, A. Ye, T. Lu, Y. Ren, Z. Xu, and K. Yuan, "Contour detection and localization of intelligent wheelchair for parking into and docking with U-shape bed," in *Proc. IEEE Int. Conf. Robot. Biomimetics*, Dec. 2011, pp. 378–383.
[7] V. DiLuoffo, W. R. Michalson, and B. Sunar, "Robot operating system 2," *Int. J. Adv. Robotic Syst.*, vol. 15, no. 3, May 2018, Art. no. 172988141877001, doi: 10.1177/1729881418770011.
[8] A. Mahphood and H. Arefi, "Tornado method for ground point filtering from LiDAR point clouds," *Adv. Space Res.*, vol. 66, no. 7, pp. 1571–1592, Oct. 2020, doi: 10.1016/j.asr.2020.06.030.
[9] D. Bolkas and A. Martinez, "Effect of target color and scanning geometry on terrestrial LiDAR point-cloud noise and plane fitting," *J. Appl. Geodesy*, vol. 12, no. 1, pp. 109–127, Jan. 2018, doi: 10.1515/jag-2017-0034.
[10] C. Dinesh, G. Cheung, and I. V. Bajic, "Point cloud denoising via feature graph Laplacian regularization," *IEEE Trans. Image Process.*, vol. 29, pp. 4143–4158, 2020, doi: 10.1109/tip.2020.2969052.
[11] P. J. Besl and N. D. McKay, "A method for registration of 3-D shapes," *IEEE Trans. Pattern Anal. Mach. Intell.*, vol. 14, no. 2, pp. 239–256, Feb. 1992, doi: 10.1109/34.121791.
[12] H. S. Shashidhara and S. Naveen Kumar, "Emphasis of LiDAR data fusion using iterative closest point and ICP registration," *Adv. Space Res.*, vol. 10, no. 1, pp. 109–127, 2020, doi: 10.19101/IJACR.2020.1048031.
[13] X. J. Shi, T. Liu, and X. Han, "Improved Iterative Closest Point (ICP) 3D point cloud registration algorithm based on point cloud filtering and adaptive fireworks for coarse registration," *Int. J. Remote Sens.*, vol. 41, no. 8, pp. 3197–3220, 2020, doi: 10.1080/01431161.2019.1701211.
[14] B. Kaleci and K. Turgut, "Plane segmentation of point cloud data using split and merge based method," in *Proc. 3rd Int. Symp. Multidisciplinary Stud. Innov. Technol. (ISMSIT)*, Oct. 2019, pp. 1–7.
[15] Y.-H. Tseng and M. Wang, "Automatic plane extraction from LIDAR data based on octree splitting and merging segmentation," in *Proc. IEEE Int. Geosci. Remote Sens. Symp. (IGARSS)*, Jul. 2005, pp. 3281–3284.
[16] M. Quan, S. Piao, M. Tan, and S.-S. Huang, "Tightly-coupled monocular visual-odometric SLAM using wheels and a MEMS gyroscope," *IEEE Access*, vol. 7, pp. 97374–97389, 2019, doi: 10.1109/ACCESS.2019.2930201.
[17] S. Karam, V. Lehtola, and G. Vosselman, "Strategies to integrate IMU and LIDAR SLAM for indoor mapping," *ISPRS Ann. Photogramm., Remote Sens. Spatial Inf. Sci.*, vols. V-1-2020, pp. 223–230, Aug. 2020, doi: 10.5194/isprs-annals-V-1-2020-223-2020.
[18] M. Doumbia, X. Cheng, and L. Chen, "A novel infrared navigational algorithm for autonomous robots," in *Proc. IEEE Int. Conf. Artif. Intell. Inf. Syst. (ICAIIS)*, Mar. 2020, pp. 20–22.
[19] I. Sung, B. Choi, and P. Nielsen, "On the training of a neural network for online path planning with offline path planning algorithms," *Int. J. Inf.*, vol. 57, Apr. 2020, Art. no. 102142, doi: 10.1016/j.ijinfomgt.2020.102142.
[20] B. Yang, Z. Ding, L. Yuan, J. Yan, L. Guo, and Z. Cai, "A novel urban emergency path planning method based on vector grid map," *IEEE Access*, vol. 8, pp. 154338–154353, 2020, doi: 10.1109/ACCESS.2020.3018729.
[21] Z. Liu, Z. Cui, Y. Li, and W. Wang, "Parameter optimization analysis of gmapping algorithm based on improved RBPF particle filter," *J. Phys., Conf. Ser.*, vol. 1646, Sep. 2020, Art. no. 012004, doi: 10.1088/1742-6596/1646/1/012004.
[22] W. A. S Norzam, H. F. Hawari, and K. Kamarudin, "Analysis of mobile robot indoor mapping using GMapping based SLAM with different parameter," *IOP Conf. Ser., Mater. Sci. Eng.*, vol. 705, Nov. 2019, Art. no. 012037, doi: 10.1088/1757-899X/705/1/012037.
[23] D. S. Pae, Y. S. Jang, S. K. Park, and M. T. Lim, "Track compensation algorithm using free space information with occupancy grid map," *Int. J. Control, Autom. Syst.*, vol. 19, no. 1, pp. 40–53, Jan. 2021, doi: 10.1007/s12555-020-0085-6.
[24] L. Xu, C. Feng, V. R. Kamat, and C. C. Menassa, "An occupancy grid mapping enhanced visual SLAM for real-time locating applications in indoor GPS-denied environments," *Autom. Construct.*, vol. 104, pp. 230–245, Aug. 2019, doi: 10.1016/j.autcon.2019.04.011.
[25] S. C. Li, C. Deng, R. Z. Sun, Q. N. Wu, and K. Y. Zhao, "Multi-path intelligent planning method based on grid division and value calculation," *IFAC Papers Online*, vol. 51, no. 17, pp. 179–184, 2018, doi: 10.1016/j.ifacol.2018.08.136.
[26] Y. L. Zhang, Y. J. An, G. Y. Wang, and X. L. Kong, "Multi motor neural PID relative coupling speed synchronous control," *Archiwum Elektrotechniki*, vol. 69, no. 1, pp. 69–88, 2020, doi: 10.24425/aee.2020.131759.
[27] N. Chen, X. M. Cai, S. Li, X. B. Zhang, and Q. H. Jiang, "Automatic extraction of rock mass discontinuity based on 3D laser scanning," *Quart. J. Eng. Geol. Hydrogeol.*, vol. 54, no. 1, pp. 2–8, 2021, doi: 10.1144/qjegh2020-054.
[28] B. Fang, G. Mei, X. Yuan, L. Wang, Z. Wang, and J. Wang, "Visual SLAM for robot navigation in healthcare facility," *Pattern Recognit.*, vol. 113, May 2021, Art. no. 107822, doi: 10.1016/j.patcog.2021.107822.
[29] Q. Zou, Q. Sun, L. Chen, B. Nie, and Q. Li, "A comparative analysis of LiDAR SLAM-based indoor navigation for autonomous vehicles," *IEEE Trans. Intell. Transp. Syst.*, early access, Mar. 18, 2021, doi: 10.1109/TITS.2021.3063477.

[30] M. Ning, M. Ren, Q. Fan, and L. Zhang, "Mechanism design of a robotic chair/bed system for bedridden aged," *Adv. Mech. Eng.*, vol. 9, no. 3, Mar. 2017, Art. no. 168781401769569, doi: 10.1177/1687814017695691.
[31] X. Z. Li, X. N. Liang, S. M. Jia, and M. A. Li, "Visual measurement based automatic docking for intelligent wheelchair/bed," *Chin. J. Sci. Instrum.*, vol. 40, no. 4, pp. 189–197, 2019, doi: 10.19650/j.cnki.cjsi.J1804420.
[32] Y. H. Li, S. Q. Zhu, Y. Q. Yu, and Z. Wang, "An improved graph-based visual localization system for indoor mobile robot using newly designed markers," *Int. J. Adv. Robotic Syst.*, vol. 15, nos. 247–267, 2018, Art. no. 1729881418769191, doi: 10.1177/1534735403256419.

YUDI ZHU (Member, IEEE) received the B.S. degree in electronic science and technology from the Henan University of Engineering, China, in 2019. She is currently pursuing the M.S. degree in biomedical engineering with the University of Shanghai for Science and Technology, China. Her research interests include trajectory planning of mobile robots and sensor information acquisition and processing.

QIAOLING MENG (Member, IEEE) received the B.S. degree from the Shenyang University of Technology, China, in 2002, the M.S. degree from Northeastern University, China, in 2008, and the Ph.D. degree from the University of Bologna, Italy, in 2012, all in mechanical engineering.

From 2012 to 2013, she held the Postdoctoral Researcher position at the University of Macau, Macau. Since 2013, she was an Assistant Professor with the University of Shanghai for Science and Technology, China, where she is currently an Associate Professor. Her current research interests include mechanical bionics, human biomechanics, and robot dynamics.

HONGLIU YU (Member, IEEE) received the B.S. degree in electrical power engineering from the Huazhong University of Science and Technology, China, in 1987, the M.S. degree in mechanical engineering from Zhengzhou University, China, in 1990, and the Ph.D. degree in industry engineering from the University of Shanghai for Science and Technology, China, in 2009.

From 1990 to 1994, he was an Assistant Professor with East China Jiaotong University, China. From 1994 to 2002, he was a Senior Mechanical Engineer and a Manager with Guangdong Jianlibao FTB Packaging Ltd., China. In 2016, he was a Senior Visiting Scholar with the Department of Computer Science, University of Hamburg, Germany. Since 2002, he has been a Professor and the Director of the Medical Instrument and Food Engineering Department, Rehabilitation Engineering and Technology Institute, University of Shanghai for Science and Technology. He is the author of six books, more than 200 academic articles, and more than 100 patents. As the charging person, he founded the first B.S. education program of rehabilitation engineering in China. His research interests include human bionic mechanics and intelligent control, rehabilitation robotics, man–machine intelligent interaction, and orthopedic devices and biomechanics.

HAITAO WANG (Member, IEEE) received the B.S. degree in electronic and information engineering from the Changshu Institute of Technology, China, in 2016. He is currently pursuing the M.S. degree in biomedical engineering with the University of Shanghai for Science and Technology, China. His research interests include computer vision and deep learning.

JIE HU (Member, IEEE) received the master's degree from the University of Shanghai for Science and Technology, in 2017. He is currently pursuing the Ph.D. degree with the Shanghai Engineering Research Center of Assistive Devices, Rehabilitation Engineering and Technology Institute, University of Shanghai for Science and Technology. He worked with Shanghai United Image Healthcare Technology Company Ltd. developed motion control systems. His current research interests include gait analysis, intelligent control of movement, and rehabilitation robotics.

PING LI (Member, IEEE) received the master's degree from the Harbin Institute of Technology, in 2013. She is currently pursuing the Ph.D. degree with the Shanghai Engineering Research Center of Assistive Devices, Rehabilitation Engineering and Technology Institute, University of Shanghai for Science and Technology. She has been working with the Chang Zhi Medical College, since 2013. Her current research interests include computer vision and rehabilitation robotics.

BINGSHAN HU (Member, IEEE) received the B.S. and M.S. degrees in electromechanical engineering and automation from the Harbin University of Science and Technology, China, in 2006, and the Ph.D. degree in mechatronic engineering from Shanghai Jiao Tong University, China, in 2010.

From 2010 to 2016, he worked as a Senior Engineer with the Shanghai Aerospace Systems Engineering Research Institute, China Aerospace Science and Technology Corporation. Since 2016, he was an Associate Professor with the University of Shanghai for Science and Technology, China. He current research interests include intelligent control of rehabilitation robot, design, modeling, and control of robot flexible drive mechanism, and lightweight cooperative service manipulator.